

Brownian Motion of Polystyrene Spheres

Jai Ranchod

Physics Department, The College of Wooster, Wooster, Ohio 44691, USA

(Dated: May 8, 2014)

This experiment is designed to use the Brownian motion of small spheres in water to measure the diameter of those spheres. A laser is shone on a glass vial containing the spheres mixed with water. The light is reflected $\pi/2$ degrees into a PMT or photo-multiplier tube. We then use a Brookhaven software program to find the intensity correlation function over a span of five minutes. We find that the correlation functions always decay exponentially with respect to the variable time step τ . We also find that as the size of the sphere increases, the rate at which the correlation between intensities decays with respect to τ decreases. We do monodisperse and polydisperse runs. The mono dispersive runs have spheres of 51 nm, 96 nm, and 304 nm while the polydisperse runs use combinations of 51 and 304 nm spheres and 96 and 304 nm spheres. For the monodisperse runs we find an average error of 35%. For the polydisperse runs we find an average error of 24%.

I. INTRODUCTION

The Brownian motion experiment is used to discover the size of particles that undergo random motion as a result of collisions with the molecules of a fluid. The phenomena of random motion was first observed with particles ejected by pollen immersed in water in 1827. Albert Einstein then explained it as resulting from the impact of water molecules on the particles. Einstein would go on to use Brownian motion to find the size of water molecules and confirm the existence of atoms. We use the same experiment to determine the size of the particles, not the water molecules.

In this experiment our particles are polystyrene spheres immersed in a vial of water. A laser is shown on the vial and the light interacts with the spheres. The light is then reflected off the spheres and into a PMT light detector facing the vial and located at a right angle to the laser.

The water molecules collide with the polystyrene spheres and bump them around in random directions. The spheres scatter the laser light, so changes in their position mean changes in the intensity distribution of the reflected light at the detector. The intensity at the detector as a function of time is therefore a reflection of how the particles are moving. How the particles move under known conditions tells us about their size.

We use intensity and electric field autocorrelation functions with a variable time step τ and the Siegert relation to form our mathematical model. These functions determine how well correlated two measured intensities are at some time interval τ away from each other. This information about correlation holds information about the size of the spheres which we can recover.

II. THEORY

We can mathematically model the intensity autocorrelation function that we would expect to see given different sized polystyrene spheres. We know how to describe the incident monochromatic light, and we can find

a probability density for the position of the polystyrene spheres. Since the spheres are what reflects the incident light, knowing these two things can bring about a description of what exactly we expect to be reflected.

We begin by considering the incident monochromatic light on the sample

$$\vec{E}_{incident} = \vec{E}_0 RE[e^{i(\omega t - \vec{k}_i \cdot \vec{r})}] \quad (1)$$

where \vec{E}_0 is the amplitude of the electric field, RE indicates the real part of the quantity, ω is the angular frequency of the electric field oscillations, \vec{k}_i is the incident wave vector, and r is the vector from the spot where the light hits a sphere to the PMT detector. Our scattered light has a similar description

$$\vec{E}_{scattered} = \vec{E}_0 RE[e^{i(\omega t - \vec{q} \cdot \vec{r})}] \quad (2)$$

where \vec{q} is defined as the scattering vector or

$$\vec{q} = \vec{k}_i - \vec{k}_s \quad (3)$$

with \vec{k}_s as the wave vector of the scattered wave. We consider this scattering to be elastic such that

$$|\vec{k}_s| = |\vec{k}_i| = \frac{2\pi}{\lambda} \quad (4)$$

where λ is the wavelength of the light. This assumption inherently includes the assumption that there is no energy lost in the scattering collisions. We know that the light is scattered at a right angle, so even though the magnitudes in Eq. 4 are equal, q will be non-zero.

Now we must briefly take a qualitative look at the Brownian motion of the polystyrene spheres in the solution. Standard Brownian motion is the random motion of a small particle immersed in a fluid. The random motion is the result of many collisions between the particle and the fluid molecules. As thermal energy causes them

to move around, the fluid molecules bombard the particle. There are many more water molecules than test particles, and the thermal motion of the water molecules is random. The bombardments of the particle are then also random, so there is no reason to expect that the particle would be bumped in one direction more than any other. Therefore, we describe the probability density for the position of the particle with a Gaussian curve given as

$$\rho(r, t) = (4\pi Dt)^{-\frac{3}{2}} (e)^{-\frac{r^2}{4Dt}} \quad (5)$$

where r is the distance of the particle from its original position, and D is the Einstein-Stokes coefficient.

The Einstein-Stokes coefficient is developed as a diffusion constant that considers friction. First, consider the Einstein diffusion coefficient for free diffusion

$$D = \frac{k_b T}{f} \quad (6)$$

where k_b is the Boltzmann constant, T is the absolute temperature, and f is the friction. The contribution from Stokes is the expansion of the friction term. Stokes found that the friction on a single particle with diameter d in a fluid of viscosity ν was

$$f = 3d\pi\nu, \quad (7)$$

thus completing the Einstein-Stokes coefficient and Eq. 5.[1]

The probability density in Eq. 5 is important because it describes the nature of the possible position of each polystyrene sphere in the fluid. The spheres scatter the light, so the position impacts how the light is scattered. This is the key point. The positions of the spheres determine how the light is scattered, and the nature of the reflection of the light determines how we think about the electric field and the intensity of the light at the detector.

We describe the normalized electric field autocorrelation function as the average of the products of all electric fields some time step τ away from each other

$$E_\tau = \frac{\langle E_r^*(t)E_r(t+\tau) \rangle}{\langle I(t) \rangle}. \quad (8)$$

With E as the electric field correlation function, I as the intensity at the light detector, and the brackets indicating the average that we use. It is important to note here that E is not an electric field, but a measure of correlation between two electric fields of varying time steps. Eq. 8 is called the normalized electric field autocorrelation function. It helps to think of

$$\tau = (n)dt \quad (9)$$

where dt is the smallest possible time step between electric field readings, and n is constant for the process that

gives one electric field correlation value, but differs for different correlation values.

Eq. 8 describes taking the electric field at time t and multiplying it by the electric field τ away. We then move to the electric field dt away, and this time value becomes the new time t . We multiply this electric field by the field at τ away, and the process is repeated throughout the entire set of time values. These products are then divided by the intensity at t . This average becomes one data point. The independent variable is τ , meaning that τ is constant for an individual data point, but different points use different τ values.

The purpose of the autocorrelation function is to describe the correlation between the electric field at time t and at time $t + \tau$. If τ is sufficiently small, then the polystyrene spheres will not have had enough time to move enough to significantly change the reflection of the light, so the detected intensity will be very similar to what it was at t . However, the larger the time interval, the more motion the Brownian particles have undergone. The motion of the spheres is random, so the change in the reflection of the light is random as well. That means that the larger τ gets, the less the intensities at t and $t + \tau$ are correlated, until finally at some point their relationship is random. The autocorrelation function is the way we determine this correlation.

We describe the intensity correlation function in a similar way to Eq. 8 using the normalized intensity autocorrelation function

$$I(\tau) = \frac{\langle I(t)I(t+\tau) \rangle}{\langle I(t) \rangle^2}. \quad (10)$$

For the rest of this paper, we will drop the description “normalized” and simply refer to Eqs. 10 and 8 as the correlation or autocorrelation functions. Again, one must remember that Eqs. 10 and 8 are measures of correlation, not intensities or electric fields.

The major key to the theoretical development of the mathematical model for Brownian motion is the Siegert relationship that relates Eqs. 8 and 10. The detector only measures intensity, which is the product of the electric field and its complex conjugate. It was initially thought that taking the complex conjugate would cause the phase information to be lost, but Siegert showed that the phase information was actually retained, showing that

$$I(\tau) = 1 + |E_\tau|^2 = 1 + ke^{-2Dq^2\tau} \quad (11)$$

thus giving us a mathematical model for what to expect for the intensity correlations of our detected light given Brownian motion in the polystyrene spheres. Here, k is a coefficient that allows us to find the best fit for our data. In the case of two sizes of polystyrene spheres being immersed in the same vial simultaneously, we only have to modify our model slightly. Notice that the exponential in Eq. 11 depends on the diameter of one polystyrene

sphere. With two different sizes of spheres, the intensity correlation function will follow a superposition of two exponential decays, each exponential term corresponding to one spheres diameter. In that case we have

$$I(\tau) = 1 + |E_\tau|^2 = 1 + ke^{-2Dq^2\tau} + k_1e^{-2D_1q^2\tau} \quad (12)$$

where D_1 is the Einstein-Stokes coefficient corresponding to the second spheres diameter.

III. PROCEDURE

The apparatus that we use for this experiment consists of a Melles-Griot He-Ne laser, a PMT light detector, and a test chamber. The test chamber is completely closed except for one hatch to insert and remove our test vials. It has a clear glass slit in the bottom for the light to enter the chamber, and another for the reflected light to escape. The vials themselves are made of glass with a plastic screw on lid and contain a mixture of polystyrene spheres and water. The entire apparatus is a product of Brookhaven Instruments.

It is also advised to label the vials with the size of the spheres that it contains simply to avoid confusion. The laser only interacts with a small portion of the bottom of the test chamber, so the test vial only needs to be a few centimeters full.

The laser is mounted on a metal rail linked to the bottom of the test chamber for stability and shines on the bottom of the test vial. The PMT is on a similar rail linked to the test chamber at a right angle to the laser. We use a right scattering angle, although this is not a necessity. Any angle will do, as long as it is well known. It is important, however, to make sure that the laser and detector are stable to ensure consistent results.

The procedure from this point experiment was relatively straightforward. The vial was put in the test chamber after it had been thoroughly wiped to remove any impurities on the surface of the glass such as fingerprints or dust. In our experiment, we mixed decahydronaphthalene ($C_{10}H_{18}$) throughout the chamber using a Brookhaven Instruments vacuum filter prior to recording data. We did this because the $C_{10}H_{18}$ has a refractive index similar to that of glass, so there would not be any distortive refractions of our monochromatic light by the $C_{10}H_{18}$. It also eliminated any air bubbles in the chamber that would have a similar distortive affect. It is not necessary to use glass and $C_{10}H_{18}$ specifically, but this is a good combination. We used the Brookhaven software program to track the intensity detected for us. This particular software program takes initial conditions into account such as the temperature of the vial and the refractive index of water. These things do have an impact on the results, so it is recommended that any program used be able to account for them. We set the program to take data from the detector for intervals of five minutes. We also did two runs with each size sphere. In

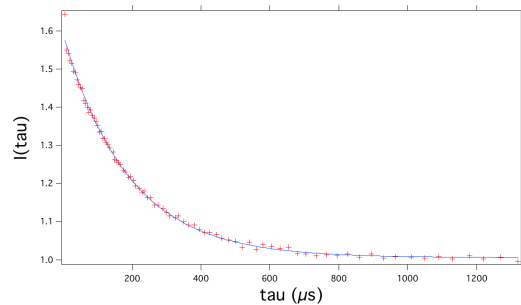


FIG. 1: Intensity correlation function for spheres size 51 nm as a function of the time step and the corresponding exponential fit. The data points (red) are fit to an exponential curve (blue).

some cases, the runs were redone as a double checking mechanism or if we suspected the data were outliers.

We have a mechanism that allowed us to control the temperature of the test chamber via water tubes. However, the link between the water tubes and the entrance to the test chamber was leaking at the time of the experiment, so the system was not used, and the temperature setting on the software program was left at room temperature.

IV. DATA ANALYSIS

The exponential fits of the intensity versus time step graphs allow us to calculate the diameter of the diffused spheres immersed in the water. The graphs we use have the intensity correlation function on the y -axis and the time step τ on the x -axis. We are therefore measuring the correlation in intensity as a function of the size of the time step. The exponential coefficient from Eq. 11 is where the information about the diameter of the spheres lies, and so the exponential fit of our data points is what we are interested in.

Each set of data is normalized to one such that the total correlation is one at all times. That is, every data point is divided by the value of the last data point, so we terminate or data set at 1. In almost all runs, there were a large amount of data points of value one. This made the graphs look like “L” shapes and therefore difficult to examine and present. We are interested in the part of the data where it changes from decreasing nearly vertically to decreasing nearly horizontally. This is what tells us the most about the change of the intensity correlation function in response to τ . Therefore, we exclude all data points that have an intensity correlation function value of less than one. Ideally there would not be any, but they are found due to noise in the system. We also exclude any function value with a τ value larger than that of the initially excluded point. This allows us to more accurately present the change in correlation function value in response to τ .

Fig. 1 shows the data points and exponential fit for

TABLE I: Size of the spheres, measured value, and percent error.

Known Sphere Size	Measured Size	Percent Error
51 nm	32.9 ± 0.82 nm	35.5%
96 nm	64.6 ± 1.4 nm	32.7%
304 nm	192.6 ± 1.6 nm	36.6%
51 nm, 304 nm	52.8 ± 8.2 nm, 197.05 ± 14.0 nm	3.5%, 35.2%
96 nm, 304 nm	73.8 ± 3.8 nm, 204 ± 9.6 nm	23.1%, 32.9%

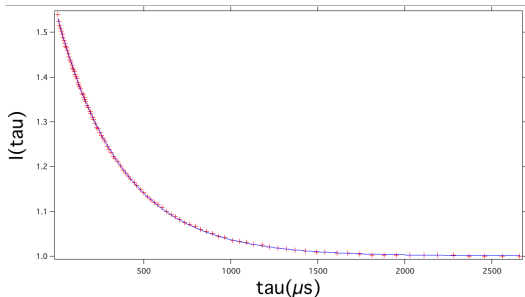


FIG. 2: A graph showing the intensity correlation function for spheres of 96 nm. The data points are red crosses and the fit line is in blue.

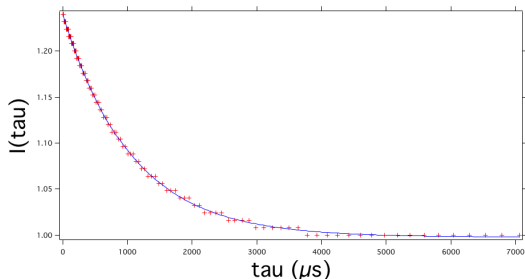


FIG. 3: A graph showing the intensity correlation function for spheres of 304 nm. The data points are red crosses and the fit line is in blue.

spheres of diameter 51 nm. We did two runs for each sized sphere, although we only show one graph for each here. Using the exponential coefficient from the fit in Igor Pro for both runs with spheres of this diameter and Eq. 11 we calculate the radius of the spheres to be 32.9 ± 0.8 nm. This was found by averaging the values calculated from each of our two runs. We will calculate all of our diameters in this way. We know that the polystyrene spheres used here have a diameter of 51 nm, yielding an error 35.5%.

Fig. 2 we see the intensity correlation function versus the time step for spheres of diameter 96 nm. Again using the exponential coefficient, we calculate the diameter of the spheres to be (64.4 ± 1.4) nm. We know that the spheres actually have a diameter of 96 nm, indicating an error of 32.7%.

Fig. 3 shows the data for the spheres of diameter 304 nm. This was the largest diameter of the spheres for a

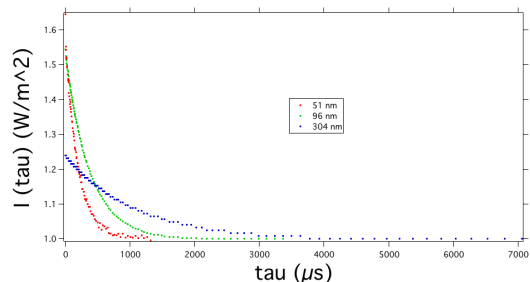


FIG. 4: Intensity correlation functions for spheres of 51 nm (red), 96 nm (green), and 304 nm (blue). Note that the larger the sphere is, the slower the decay of the correlation.

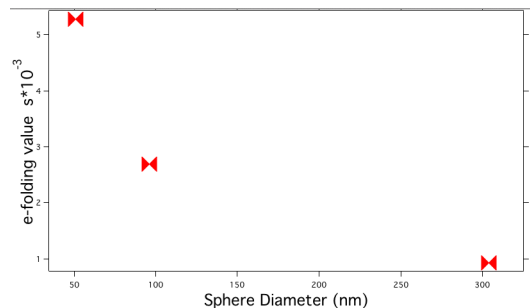


FIG. 5: Exponential fit coefficient values of various curves versus the size of the corresponding polystyrene spheres.

monodisperse solution that we used. We calculate the diameter here to be 191 ± 0.02 nm. This means we have an error of 37.3%. Also notice from Fig. 4 that as the diameter of the spheres increases, the intensity correlation function flattens out.

This phenomena is shown in Fig. 4. Graphically we can see that this implies that the smaller a sphere is, the less correlation there is between intensity values. This makes sense because the larger a sphere is, the more inertia it will have. Therefore, if two spheres are bombarded the same amount by the water molecules, the smaller of the two will move more in the same time interval because it has less inertia to resist moving. More movement by one size of sphere than the other in an equal time interval means the intensity will correlate less after light reflects off the smaller spheres.

Fig. 5 shows the exponential coefficient values of certain exponential fits and the size of sphere that the fit

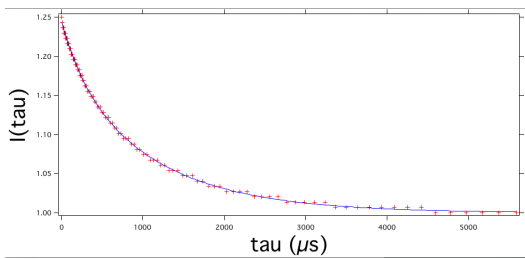


FIG. 6: Intensity correlation functions for spheres of 51 nm and 304 nm in the same vial. The data points are red crosses, and the fit curve is in blue.

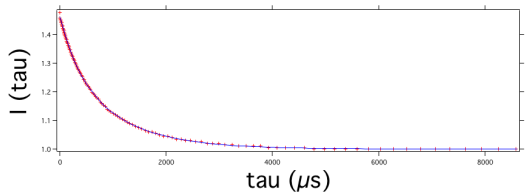


FIG. 7: Intensity correlation functions for spheres of 96 nm and 304 nm in the same vial. The data points are red crosses, and the fit curve is in blue.

corresponds to. As shown in Eq. 11 the exponential coefficient which we choose to name α for this experiment is

$$\alpha = -2Dq^2. \quad (13)$$

This value is a measure of how fast the exponential fit decays. In Fig. 5 we see that as the size of the spheres increases, the exponential coefficient decreases as previously mentioned.

We also used polydisperse samples, meaning we mixed two sizes of spheres in the same vial. We used a combination of 51 nm spheres and 304 nm spheres, as well as a combination of 96 nm spheres and 304 nm spheres. When calculating the diameter of these spheres, we must use Eq. 12 for the fit because each exponential coefficient holds the information for one diameter. Two diameters being used therefore calls for two exponential terms. For the combination of 51 nm and 304 nm spheres we find the diameters to be 53 ± 8 nm and 197 ± 14 nm respectively. For the 51 nm spheres we find an error of 3.5% and for the spheres of 304 nm we find an error of 35%.

The graph of the data for the combination of spheres of 51 nm and 304 nm is shown in Fig. 6.

We also have a polydisperse mixture of 96 nm spheres and 304 nm spheres. In this case we find the spheres to

be of sizes 74 ± 3.8 nm and 204 ± 10 nm respectively. These have corresponding errors of 23% and 33%, again respectively.

The graph of the data for the combination of spheres of 96 nm and 304 nm is shown in Fig. 7.

Notice that in every case so far, the data points have decreased in a well formed exponential curve as a function of τ . This is exactly what we would expect given Eqs. 11 and 12.

The errors in this experiment could be due to the unique features of the PMT detector. The detector we use is a high precision instrument, meaning that any calibrations and preset conditions are highly sensitive. If any initial condition or parameter is incorrect, this could cause a significant amount of error.

One other potential source of error is the fact that the detector was tilted slightly away from the primary reflection in order to avoid excessive noise being brought into the PMT. That is, the reflection was close to 90 degrees, but was not exactly. Adjusting the position of the tube solves the initial problem, but also creates potential error in the results.

V. CONCLUSION

In this experiment we conclude that the smaller a sphere is, the less correlation there is between intensity values. We make this conclusion because the intensity correlation functions become flatter as the size of the sphere increases. That means that the derivative of the curve on the portion that we examine becomes smaller as the size of the spheres increases. We conclude that this is a result of the larger spheres having more inertia and therefore being more resistive to the motion that would cause lack of correlation in intensities from reflected light. We also find the diameters of the spheres we use to be those found in table I. These correspond to known sphere diameters of 51 nm, 96 nm, 304 nm, 51 nm and 304 nm, 96 nm and 304 nm respectively. We find that the intensity correlation function fits to a decreasing exponential in every case. This means that as the time step τ increases, the correlation of the intensity at $t + \tau$ to the intensity at t decreases exponentially. We also notice that this fits our model perfectly. We finally conclude that the error in this experiment is associated with either the sensitive initial parameters and settings of the PMT detector or the fact that the detector was intentionally tilted away from the main area of reflected intensity.

-
- [1] *Standard Brownian Motion*, accessed 2/27/2014 <http://www.math.uah.edu/stat/brown/Standard.html>
 [2] C. Svanberg, R. Bergman *Photon Correlation Spectroscopy* accessed 2/27/2014 (Chalmers University of Tech-

- nology, 2005) http://fy.chalmers.se/~f1xjk/TIF060/home_files/pcstheo.pdf
 [3] *Light Scattering* accessed 2/28/2014 <http://mxp.physics.umn.edu/s02/Projects/LightScattering/>

theory.htm

[4] *Understanding Autocorrelation in Time* accessed 4/14/2009 (FCS Expert Solutions)

<http://www.fcsexpert.com/classroom/theory/what-is-autocorrelation.html>